Chemical Engineering Journal 450 (2022) 138179

Contents lists available at ScienceDirect

Chemical Engineering Journal

journal homepage: www.elsevier.com/locate/cej

Unleashing lignin potential through the dithionite-assisted organosolv fractionation of lignocellulosic biomass

Filippo Brienza [a,b], Korneel Van Aelst [c], François Devred [b], Delphine Magnin [b], Maxim Tschulkow [d,e], Philippe Nimmegeers [d,e,f], Steven Van Passel [d,e,g], Bert F. Sels [c], Patrick Gerin [a], Damien P. Debecker [b,*], Iwona Cybulska [a,*]

[a] Earth and Life Institute (ELI), UCLouvain, Croix du Sud 2, 1348 Louvain-La-Neuve, Belgium
[b] Institute of Condensed Matter and Nanoscience (IMCN), UCLouvain, Place Louis Pasteur 1, 1348 Louvain-La-Neuve, Belgium
[c] Centre for Sustainable Catalysis and Engineering, KU Leuven, Celestijnenlaan 200F, 3001 Leuven, Belgium
[d] University of Antwerp, Department of Engineering Management, Prinsstraat 13, 2000 Antwerpen, Belgium
[e] VCCM, Flanders Make
[f] Intelligence in Processes, Advanced Catalysts and Solvents (iPRACS), Faculty of Applied Engineering, University of Antwerp, Groenenborgerlaan 171, 2020 Antwerp, Belgium
[g] Nanolab Centre of Excellence, Prinsstraat 13, 2000, Antwerp, Belgium

ARTICLE INFO

Keywords:
Lignocellulose
Biorefinery
Organosolv
Dithionite
Lignin depolymerization

ABSTRACT

The development of biomass pretreatment approaches that, next to (hemi)cellulose valorization, aim at the conversion of lignin to chemicals is essential for the long-term success of a biorefinery. Herein, we discuss a dithionite-assisted organosolv fractionation (DAOF) of lignocellulose in *n*-butanol and water to produce cellulosic pulp and mono-/oligo-aromatics. The study frames the technicalities of this biorefinery process and relates them to the features of the obtained product streams. We comprehensively identify and quantify all products of interest: solid pulp (acid hydrolysis-HPLC, ATR-FTIR, XRD, SEM, enzymatic hydrolysis-HPLC), lignin derivatives (GPC, GC–MS/FID, 1H–13C HSQC NMR, ICP-AES), and carbohydrate derivatives (HPLC). These results were used for inspecting the economic feasibility of DAOF. In the best process configuration, a high yield of monophenolics was reached (~20 wt%, based on acid insoluble lignin in birch sawdust). Various other lignocellulosic feedstocks were also explored, showing that DAOF is particularly effective on hardwood and herbaceous biomass. Overall, this study demonstrates that DAOF is a viable fractionation method for the sustainable upgrading of lignocellulosic biomass.

1. Introduction

The use of lignocellulose for the sustainable production of energy, chemicals or materials was recognized as a promising alternative to fossil resources [1–5]. As a composite biopolymer, lignocellulose is constituted of three main components: cellulose, hemicellulose and lignin, which are linked together to form a deeply intertwined structure. The high heterogeneity of this substrate, and the related recalcitrance toward bioprocessing [8], imposed the adoption of an initial pretreatment in biorefineries, aimed at reducing the complexity of the initial feedstock by disassembling lignocellulose structure [6,7] before further conversion of the intermediates toward valuable end products (*e.g.* paper, bioethanol [8] levulinic acid [9] 5-HMF [10] furfural [10] phenol [11,12] bionaphta [13], etc.). While several methods were developed for the pretreatment of lignocellulosic biomass, the vast majority of them focused almost exclusively on the valorization of the carbohydrate fraction of lignocellulose [14,15]. From this point of view, the need for efficient strategies to convert lignin into value-added products still constitutes a paramount challenge for biorefineries [16–18]. Throughout the last few decades, a broad variety of processes were studied for the valorization of the technical lignin fractions obtained upon biomass pretreatment, but their typically degraded structure hampered their upgrading toward aromatic chemicals [19–21].

Recently, a novel biorefining concept, targeting lignin depolymerization in the frame of biomass pretreatment, received increasingly higher attention in the scientific community. This so-called "lignin-first"

* Corresponding authors.
E-mail addresses: damien.debecker@uclouvain.be (D.P. Debecker), iwona.cybulska@uclouvain.be (I. Cybulska).

https://doi.org/10.1016/j.cej.2022.138179
Received 29 April 2022; Received in revised form 15 July 2022; Accepted 16 July 2022
Available online 20 July 2022
1385-8947/© 2022 Elsevier B.V. All rights reserved.

approach offers the opportunity to achieve a more complete valorization of lignocellulose components, with an excellent preservation of their chemical functionalities [22–25]. Among the different methodologies that were proposed for lignin-first pretreatment, reductive catalytic fractionation (RCF) is particularly promising, as it allows to simultaneously isolate lignin from a carbohydrate pulp with high yields of delignification (up to about 90 wt% of lignin in the initial biomass) and to convert it toward valuable monophenolics with near-theoretical yields (based on the content of β-O-4 linkages in the lignin matrix) [25,26]. In spite of these inherent advantages, the use of precious metal catalyst and high pressures of hydrogen gas employed within RCF represent important limitations, imposing considerable processing costs, as well as strict safety and equipment requirements [26,27] The mechanism underlying RCF was elucidated in a study by Van den Bosch *et al.*, who showed that lignin is extracted from biomass by solvolysis and labile ether bonds in lignin structures (predominantly β-O-4 linkages) [3] undergo reductive cleavage with the formation of reactive lignin units. The latter are ultimately stabilized against recondensation by catalytic hydrogenation of C═C bonds within their (hydroxy)alkenyl side chains [28] A reductive cleavage of β-O-4 bonds was demonstrated to occur as well in a study conducted by Klinger *et al.* on the use of nucleophilic thiols for the depolymerization of pre-extracted, oxidized lignin, in which the authors reported a substantial production of monophenolics [29,30] This process was explored further by Fang *et al.*, who developed an elegant thiol-assisted electrolytic approach for reductive lignin depolymerization [31].

Inspired by these works, we recently reported the proof of concept for enhancing the reductive depolymerization of lignin through the use of sodium dithionite ($Na_2S_2O_4$), an inexpensive and widely available sulfur-based reducing agent, as an alternative to precious metals and hydrogen gas, or nucleophilic thiols [32,33] Such dithionite-assisted organosolv fractionation (DAOF) was shown to achieve superior conversion of lignin toward valuable monophenolics compared to a standard organosolv process, while concomitantly yielding a highly digestible cellulosic pulp. Moreover, the adoption of a *n*-butanol–water solvent combination conveniently facilitates product separation. Importantly, we demonstrated that the use of sodium dithionite triggers the reductive cleavage of β-O-4 bonds in lignin and the hydrogenation of unsaturated side chains in the generated phenolic units [32].

Herein, we target an in-depth understanding of the phenomena governing lignocellulose disassembly and lignin depolymerization during the DAOF by investigating the influence of process conditions on the features of the isolated product streams. The experimental results are used to assess the techno-economic feasibility of the DAOF, and to identify the configuration which maximizes the process profitability, highlighting the current limitations and the potential pathways for the future improvements of this technology. Furthermore, the flexibility of the DAOF with respect to the treatment of various biomass feedstocks is inspected (including hardwood, softwood, and herbaceous feedstocks). We argue that the DAOF represents an attractive strategy to implement lignin valorization within biomass pretreatment, for a sustainable production of low-molecular weight phenolics.

2. Materials and methods

A full list of the materials used in this work and detailed descriptions of the experimental procedures and of the calculations performed are available in the Supporting Information. Here, a condensed description of the main experimental process is provided.

2.1. Fractionation experiments

DAOF experiments were carried out in duplicates in a 300 mL Parr batch reactor (Fig. S1, Parr Instrument Company, Moline, IL, U.S.): a chosen amount of biomass (3–12 g) was introduced in the reactor, together with 120 mL of a *n*-butanol–water mixture (*n*-butanol content: 0–100 % v/v) and sodium dithionite (loading: 0 %–33 % w/$w_{biomass}$). The air in the reactor was displaced by flushing with N_2, then the reactor was pressurized with N_2 (1 or 30 bar). The impeller speed was set to 750 rpm and the temperature was increased at a rate of about 10 °C min^{-1}, up to a setpoint comprised between 150 °C and 250 °C. Once the setpoint was reached, the mixture was left to react at constant temperature for a duration of 0 to 6 h.

2.2. Products separation and analysis

After each experiment, the reactor was quickly cooled down to ambient temperature by letting water flow through the cooling coil, depressurized, and its content was collected. A solid and a liquid fraction were separated by centrifugation. The solid fraction was washed first with pure *n*-butanol (15 mL $g^{-1}_{initial\ biomass}$) and then with pure water (15 mL $g^{-1}_{initial\ biomass}$) to remove apolar and polar components weakly adsorbed to the pulp. Subsequently, the washing solvents were combined with the liquid fraction, and the mixture was filtered to eliminate residual solid particles. The filtrate was transferred to a separating funnel, where it separated into an organic and an aqueous liquid phase (Fig. S2a), which were then separately collected. The retentate was recovered and added to the solid fraction, before drying the solids at 60 °C to a constant weight.

Dry matter, ash, and organic matter contents were determined for all the isolated fractions.

The solid fraction (Fig. S2b) was characterized via a battery of techniques, including acid/enzymatic hydrolysis followed by high-performance liquid chromatography (HPLC) analysis, attenuated total reflection-Fourier transform infrared spectroscopy (ATR-FTIR), X-ray powder diffraction (XRD) analysis, field emission gun scanning electron microscopy (FEG-SEM).

Portions of the organic liquid fraction were evaporated under nitrogen flow to remove the solvent, then underwent a threefold liquid–liquid extraction with dichloromethane and water, to isolate lignin derivatives from more polar products. The dichloromethane fractions were mixed, and the solvent was evaporated under vacuum to yield a viscous brown lignin oil (Fig. S2c), which was subsequently analyzed via gel permeation chromatography (GPC), gas chromatography (GC) coupled with a mass spectrometry (MS) detector and a flame ionization detector (FID), and $^{1}H–^{13}C$ heteronuclear single quantum coherence (HSQC) nuclear magnetic resonance (NMR). Extraction of monophenolics from the organic fraction was performed by evaporating the solvent of a portion of the organic fraction under nitrogen flow, then subjecting the non-volatile residue to a sixfold liquid–liquid extraction with cyclohexane and water. Mixing the cyclohexane fractions and evaporating the solvent under vacuum yielded a monomers-rich cyclohexane oil, which was characterized via GPC and GC–MS/FID. Additionally, the sulfur content of the organic fraction and of the cyclohexane oil was assessed by inductively coupled plasma atomic emission spectroscopy (ICP-AES).

The pH of the aqueous liquid fraction was measured, and the non-condensed carbohydrate derivatives present in this fraction were quantified by HPLC.

3. Results and discussion

3.1. Dithionite-assisted organosolv fractionation: Process outline

In order to determine the outcomes of different process configurations, unless otherwise specified, batch experiments were carried out in duplicates treating birch sawdust (*Betula pendula,* particle size ≤ 2 mm [34] biomass composition reported in Table S1) in a mixture of *n*-butanol and water, at temperatures in a range between 150 and 250 °C, in the presence of different loadings of sodium dithionite, under different pressures of N_2. After the fractionation, a cellulose-rich solid pulp was recovered. Concomitantly, two liquid fractions were obtained:

an organic fraction, comprising lignin derivatives and soluble humins, and an aqueous fraction, containing non-condensed carbohydrate derivatives (*e.g.* mono- and oligosaccharides, polyols and organic acids). An overview of the DAOF process is shown in Fig. 1.

With the goal of improving the performance of the DAOF of lignocellulosic biomass, we investigated the influence of different variables on the properties of the obtained fractions, including the operating temperature, the exogenous nitrogen pressure, the loading of sodium dithionite, the solvent/biomass ratio, the reaction time, and the *n*-butanol/water ratio.

3.2. Lignocellulose disassembly and solubilization

The influence of process conditions on the solvolytic disassembly of lignocellulose was inspected by assessing the mass balance of organic matter (OM) with respect to the different fractions recovered (Fig. 2 and Table S2). While the nitrogen pressure (Fig. 2b and Table S2, entries 3, 6), the loading of dithionite (Fig. 2c and Table S2, entries 3, 7–9) and the solvent/biomass ratio (Fig. 2d and Table S2, entries 9–11) did not appear to substantially affect lignocellulose solubilization, the operating temperature, the reaction time and the *n*-butanol/water ratio were recognized as key parameters in driving the solvolytic disassembly of biomass.

Consistently with previous findings on hydrothermal and organosolv pretreatments [35,36], increasing the temperature was found to promote the solubilization of lignocellulose components during the DAOF, with a recovery of OM in the pulp that diminished from 81 wt% of OM in the initial biomass at 150 °C to 10 wt% at 250 °C (Fig. 2a and Table S2, entries 1–5). Analogously, extending the contact time from 0 h (*i.e.* reaction halted as soon as the setpoint temperature was reached) to 6 h resulted in a diminution of the recovery of OM in the pulp from 76 wt% to 40 wt%, accompanied by a gradual increase of the recovery of OM in the liquid fraction (Fig. 2e and Table S2, entries 9, 12–14). Notably, the mass balance for OM was below 100 wt% at temperatures greater than 150 °C and reaction times longer than 0 h, indicating an increasingly larger conversion of lignocellulose toward volatile components under more severe conditions (*e.g.* conversion of C5 and C6 polysaccharides toward furans, formic acid, and CO_2) [37–39].

The *n*-butanol/water ratio was also found to affect the recovery of OM in the pulp, which decreased from 65 wt% in pure *n*-butanol to 44 wt % upon addition of water, and was determined to be 53 wt% in water alone, highlighting the synergetic effect of the *n*-butanol–water mixture with respect to lignocellulose disassembly (Fig. 2f and Table S2, entries 9, 15–18). Correspondingly, the recovery of OM in the liquid fraction was maximized when *n*-butanol and water were employed together. These observations can be explained by the dual nature of the solvent: on the one hand, *n*-butanol is more apolar than water and is less active toward solvolysis [40] on the other hand, it possesses a higher ability to solubilize lignin and humins compared to water [41,42]. Interestingly, the mass balance was not affected by the *n*-butanol/water ratio, indicating that the formation of volatile products does not depend on this parameter.

3.3. Solid fraction: Cellulosic pulp

The isolated solid fractions were subjected to acid hydrolysis, following a well-established procedure [43], and their composition in terms of polysaccharides and lignin was determined (Table 1). Furthermore, the chemical and structural features of the different pulps, their cellulose crystallinity index (CI) [44], and their surface morphology were analyzed *via* ATR-FTIR spectroscopy (spectra reported in Fig. S3, band assignments in Table S3), XRD analysis (Fig. S4) and SEM (Figs. S5–S8), respectively. Additionally, the effectiveness of the pretreatment with respect to enhancing the processability of the solid fractions was evaluated by assessing the enzymatic digestibility of the preserved C5 and C6 polysaccharides (mainly xylan and glucan) toward monosaccharides (xylose and glucose) (Fig. 3) [45]. Except for nitrogen pressure (Table 1, entries 3, 6 and Fig. 3b) and for the loading of sodium dithionite (Table 1, entries 3, 7–9 and Fig. 3c), all the considered process variables were found to exert an influence on the retention of polysaccharides, on delignification, and on the pulp processability.

At a low treatment temperature of 150 °C most of the polysaccharides were found to be preserved in the pulp, with recoveries of C5 and C6 polysaccharides of 83 wt% and 93 wt%, respectively (Table 1, entry 1). A lignin recovery of 128 wt% was measured in the solid fraction. Such increase of lignin content may be ascribed to the presence of non-removed extractives in the pulp [46], or to the partial formation of pseudolignin (*e.g.* insoluble humins) and its deposition on cellulose fibers [47–49]. Processing at higher temperatures triggered the removal of hemicellulose and lignin (Table 1, entries 2–5), whereas the recovery of C6 polysaccharides remained rather constant up until 200 °C, above which cellulose hydrolysis increased markedly. These observations were confirmed by FTIR analyses of the solid fractions (Fig. S3a), which showed that incrementing the treatment temperature above 150 °C resulted in the gradual disappearance of the bands at 1235, 1465, 1510, 1595, and 1740 cm^{-1}, assigned to lignin and hemicellulose [50–53], pointing out their removal from the pulps. On the other hand, for the solid fraction isolated after a treatment at 250 °C, a more marked band appeared at 1045 cm^{-1} in the FTIR spectrum (assigned to lignin) [54], pinpointing the presence of a higher content of residual lignin relative to

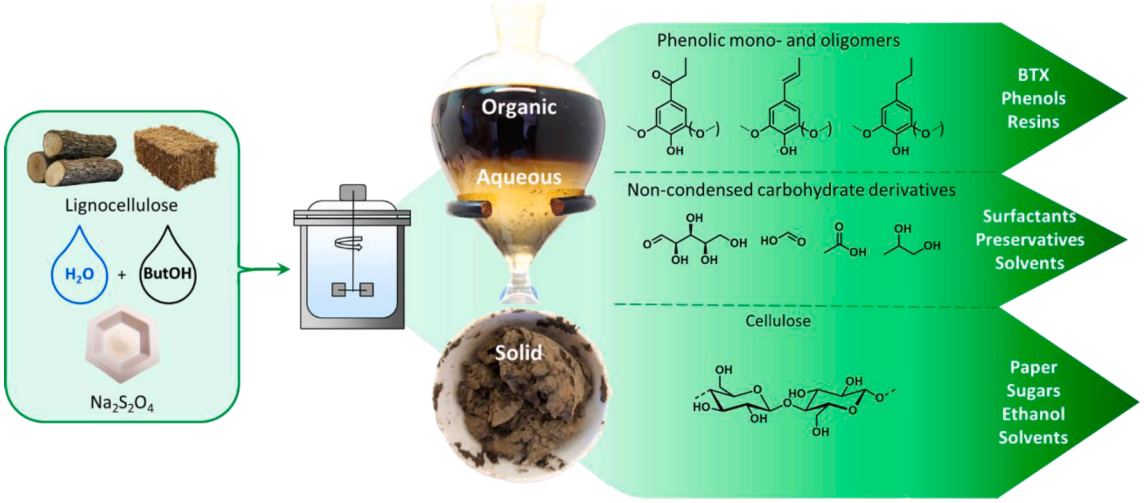


Fig. 1. Outline of the dithionite-assisted organosolv fractionation of lignocellulosic biomass, with possible valorization routes for each product stream.

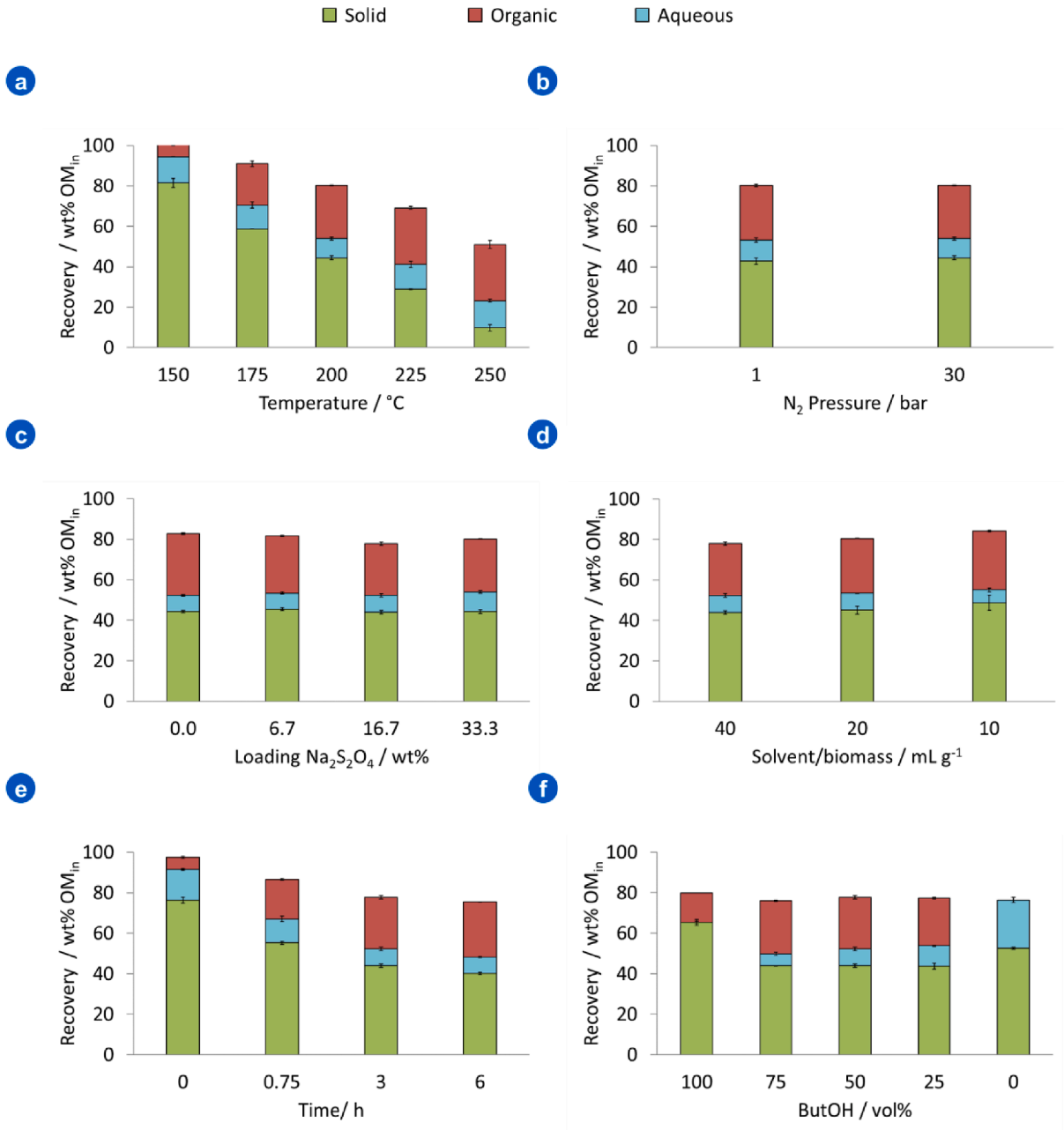


Fig. 2. Recovery of organic matter in the solid and liquid (organic and aqueous) fractions obtained after the DAOF of birch sawdust carried out at different operating temperatures (a), exogenous pressures (b), loadings of $Na_2S_2O_4$ (c), solvent/biomass ratios (d), reaction times (e), and *n*-butanol/water ratios (f). Unless otherwise specified, fractionation experiments were performed treating 3 g of birch sawdust in 120 mL of an equivolumetric mixture of *n*-butanol and water, at 200 °C, under 30 bar of N_2 (introduced at ambient temperature), in the presence of $Na_2S_2O_4$ (33.3 % w/$w_{biomass}$ for panels a and b; 16.7 % w/$w_{biomass}$ for panels d–f), for a duration of 3 h.

the amount of pulp isolated after severe treatment. Notably, the bands at 1160 cm^{-1} and 1098 cm^{-1} became more evident at higher temperatures, revealing a larger cellulose purity and a higher proportion of crystalline cellulose [52,53]. Further XRD analyses of the pulps showed that their CIs increased with temperature from 42 % at 150 °C to 56 % at 225 °C (Fig. 3a), owing to the removal of amorphous components (lignin and hemicellulose) from the solid fraction [55,56]. Remarkably, the pulp isolated at 150 °C possessed a CI lower than that of raw biomass. Such finding may be explained by the residual presence of extractives in the pulp, or by the redeposition of pseudolignin on cellulose fibers, which are known to negatively affect the CI [46,55]. SEM images of the raw biomass and of the solid fractions revealed that increasing the treatment temperature resulted in a gradually smoother surface and in the appearance of bundles of fibers that became thinner as the temperature was raised (Fig. S5a–d). This indicates a partial disassembly of the fibrous structure, which is expected to enhance the enzymatic digestibility of the pulp [57]. In agreement with this, a larger convertibility of glucan and xylan was determined for the pulps obtained at higher temperatures (Fig. 3a), reaching yields of saccharification greater than 90 % above 175 °C, by virtue of an enhanced delignification and a higher accessibility of cellulose fibers.

The adoption of lower solvent/biomass ratios resulted in a gradual diminution of the recovery of C5 and C6 polysaccharides, from 20 wt% and 92 wt% at 40 mL g^{-1} down to 11 wt% and 82 wt%, respectively, at 10 mL g^{-1} (Table 1, entries 9–11). The intermediates produced by carbohydrate degradation, including short organic acids [37,38,58], may

Table 1
Biomass derivatives obtained for the DAOF of birch sawdust under varying process conditions.

Entry	Experimental conditions[a]						Solid Recovery[b] (wt%)			Organic Yield[c] (wt%)		Aqueous Yield[d] (wt%)
	T (°C)	P_{N2} (bar)	$Na_2S_2O_4$ (wt%)[e]	S/B[f] (mL g^{-1})	t (h)	ButOH (vol%)	C5	C6	Lignin	Oil	Mono	C5, C6 derivatives
1	150	30	33.3	40	3	50	83 ± 5	93 ± 2	128 ± 7	4 ± 1	1.2 ± 0.4	0.1 ± 0.0
2	175	30	33.3	40	3	50	43 ± 2	92 ± 3	77 ± 8	63 ± 1	5.9 ± 1.2	2.8 ± 0.2
3[g]	200	30	33.3	40	3	50	18 ± 3	92 ± 1	28 ± 3	93 ± 7	18.1 ± 1.7	7.5 ± 0.4
4	225	30	33.3	40	3	50	5 ± 2	68 ± 1	21 ± 6	121 ± 6	17.1 ± 2.5	2.8 ± 0.2
5	250	30	33.3	40	3	50	–	21 ± 7	11 ± 2	131 ± 7	11.2 ± 0.8	7.5 ± 0.4
6	200	1	33.3	40	3	50	15 ± 2	93 ± 2	27 ± 9	92 ± 2	17.7 ± 2.3	5.7 ± 0.3
7[g]	200	30	0.0	40	3	50	16 ± 1	93 ± 3	31 ± 9	95 ± 2	3.6 ± 0.6	3.4 ± 0.5
8	200	30	6.7	40	3	50	20 ± 2	91 ± 2	36 ± 2	90 ± 6	12.1 ± 1.3	2.6 ± 0.5
9	200	30	16.7	40	3	50	20 ± 2	92 ± 2	27 ± 3	93 ± 6	19.4 ± 1.8	4.0 ± 0.4
10	200	30	16.7	20	3	50	9 ± 4	88 ± 5	54 ± 5	99 ± 1	18.2 ± 1.2	3.2 ± 0.5
11	200	30	16.7	10	3	50	11 ± 1	82 ± 4	66 ± 6	119 ± 2	16.7 ± 1.0	4.3 ± 0.4
12	200	30	16.7	40	0[h]	50	68 ± 5	93 ± 2	119 ± 5	10 ± 0	0.4 ± 0.2	0.5 ± 0.2
13	200	30	16.7	40	0.75	50	42 ± 3	95 ± 2	54 ± 7	59 ± 5	9.9 ± 1.3	2.3 ± 0.5
14	200	30	16.7	40	6	50	9 ± 2	87 ± 5	26 ± 7	115 ± 5	20.6 ± 2.1	3.7 ± 0.8
15	200	30	16.7	40	3	100	69 ± 4	89 ± 3	69 ± 6	63 ± 5	6.6 ± 2.2	1.7 ± 0.4[i]
16	200	30	16.7	40	3	75	24 ± 2	89 ± 1	34 ± 3	96 ± 7	16.8 ± 1.6	3.5 ± 0.1
17	200	30	16.7	40	3	25	13 ± 1	94 ± 1	31 ± 6	84 ± 5	18.2 ± 1.8	2.6 ± 0.1
18	200	30	16.7	40	3	0	6 ± 0	80 ± 4	107 ± 4	44 ± 5[j]	4.1 ± 1.1[j]	2.5 ± 0.6

[a] Reactions were carried out in duplicates.
[b] Recovery of hemicellulose, cellulose, and acid-insoluble lignin in the solid fraction, expressed with respect to the weights of the different components in the initial biomass.
[c] Yield of lignin oil and phenolic monomers in the organic fraction, expressed with respect to the weight of acid-insoluble lignin contained in the initial biomass.
[d] Yield of non-condensed carbohydrate derivatives in the aqueous fraction, expressed with respect to the total weight of polysaccharides contained in the initial biomass.
[e] Expressed with respect to the weight of biomass introduced in the reactor.
[f] Solvent/biomass ratio.
[g] Experimental conditions investigated in our previous work [32].
[h] Fractionation halted immediately after the setpoint temperature was reached.
[i] Determined in the organic fraction. [j] Determined in the aqueous fraction.

be responsible for promoting further (hemi)cellulose decomposition. At the same time, higher recoveries of lignin were measured, which may be due to a poorer lignin solvolysis (arising from an increased mass transfer resistance at higher biomass concentration) [59] or to pseudolignin formation. A larger presence of lignin at lower solvent/biomass ratios was recognized also *via* FTIR analyses, with the bands at 1045 cm^{-1} and 1595 cm^{-1} that were more apparent at 10 mL g^{-1} (Fig. S3d). However, we cannot exclude the contribution of furanic species which would be associated with IR bands in the same regions (*e.g.* 1600 and 1020 cm^{-1}) [64]. The band at 1098 cm^{-1} was also more evident at low solvent/biomass ratio, indicating a larger content of crystalline cellulose in the pulp [53]. XRD analyses revealed that no major change occurred in the CIs of the pulps obtained at different solvent/biomass ratios (Fig. 3d). Such observation may be explained by the opposed effects that an increased content of amorphous (pseudo)lignin and a higher fraction of crystalline cellulose would exert on the CI [60]. SEM images of the solid fractions showed that the adoption of low solvent/biomass ratios resulted in a rougher, more tightly packed fibrous structure (Fig. S6a–c), possibly less susceptible toward enzymatic conversion [35]. Consistently, the digestibility of glucan was found to decrease from 91 % at 40 mL g^{-1} to 77 % at 10 mL g^{-1} (Fig. 3d), suggesting that the higher content of (pseudo)lignin and the more compact structure observed at higher loading limits cellulose accessibility for enzymatic attack [35,49].

Increasing the reaction time had a similar impact as raising the operating temperature (Table 1, entries 9, 12–14). While high recoveries of polysaccharides (68 wt% for C5 and 93 wt% for C6) and pseudolignin formation (lignin recovery of 119 wt%) were observed at short reaction times (*i.e.* "0 h" condition), longer treatment durations resulted in the extensive removal of hemicellulose and lignin. These observations were substantiated by FTIR analyses of the solid fractions (Fig. S3e), which showed that minor changes in the spectrum were apparent at short reaction times compared to the raw biomass, whereas longer processing times resulted in the disappearance of the bands at 1235 cm^{-1}, 1465 cm^{-1}, 1510 cm^{-1}, and 1740 cm^{-1}, assigned to lignin and hemicellulose [50–53], and in the shrinkage of the band at 1595 cm^{-1}, assigned to lignin [53]. The higher purity of cellulose at longer reaction times was highlighted by the gradually more apparent band at 1160 cm^{-1} [52]. In agreement with such findings, the CIs of the pulps increased with time from 44 % at 0 h up to 53 % at 6 h (Fig. 3e). SEM analyses showed that the surface of the solid fraction isolated after 0 h of treatment possessed a coarse morphology, much alike that of the raw biomass, and no fibers were apparent (Fig. S7a, b). Conversely, after 3 h a more open fibrous structure was observed (Fig. S7c). Accordingly, the digestibility of glucan and xylan increased with the reaction time, and values greater than 90 % were measured for the pulps obtained after processing for 3 h or longer (Fig. 3e).

The effect of the *n*-butanol/water ratio on the properties of the isolated pulps confirmed the benefits deriving from the adoption of a mixture of *n*-butanol and water compared to the pure solvents (Table 1, entries 9, 15–18). When *n*-butanol was employed alone, only a marginal removal of hemicellulose and lignin from the pulp was observed (31 wt % for both components), whereas the introduction of water led to an improved solubilization of these components, and a sharp increase of cellulose purity in the pulp (up to 77 wt%, relative to the DM content of the solid fraction). The use of water alone led to extensive removal of C5 polysaccharides and a marginal decrease of the recovery of C6 polysaccharides, along with the formation of pseudolignin (lignin recovery of 107 wt%), highlighting how a solvent that is too polar would not be convenient for the DAOF, as it would lack the ability to solubilize lignin and humic products formed during the fractionation. FTIR analyses of the solid fractions showed that a treatment in pure *n*-butanol led to a decrease of the bands at 1235 cm^{-1} and 1510 cm^{-1} and to the disappearance of the band at 1740 cm^{-1}, assigned to hemicellulose and lignin (Fig. S3f) [50–53]. On the other hand, the introduction of water as a co-

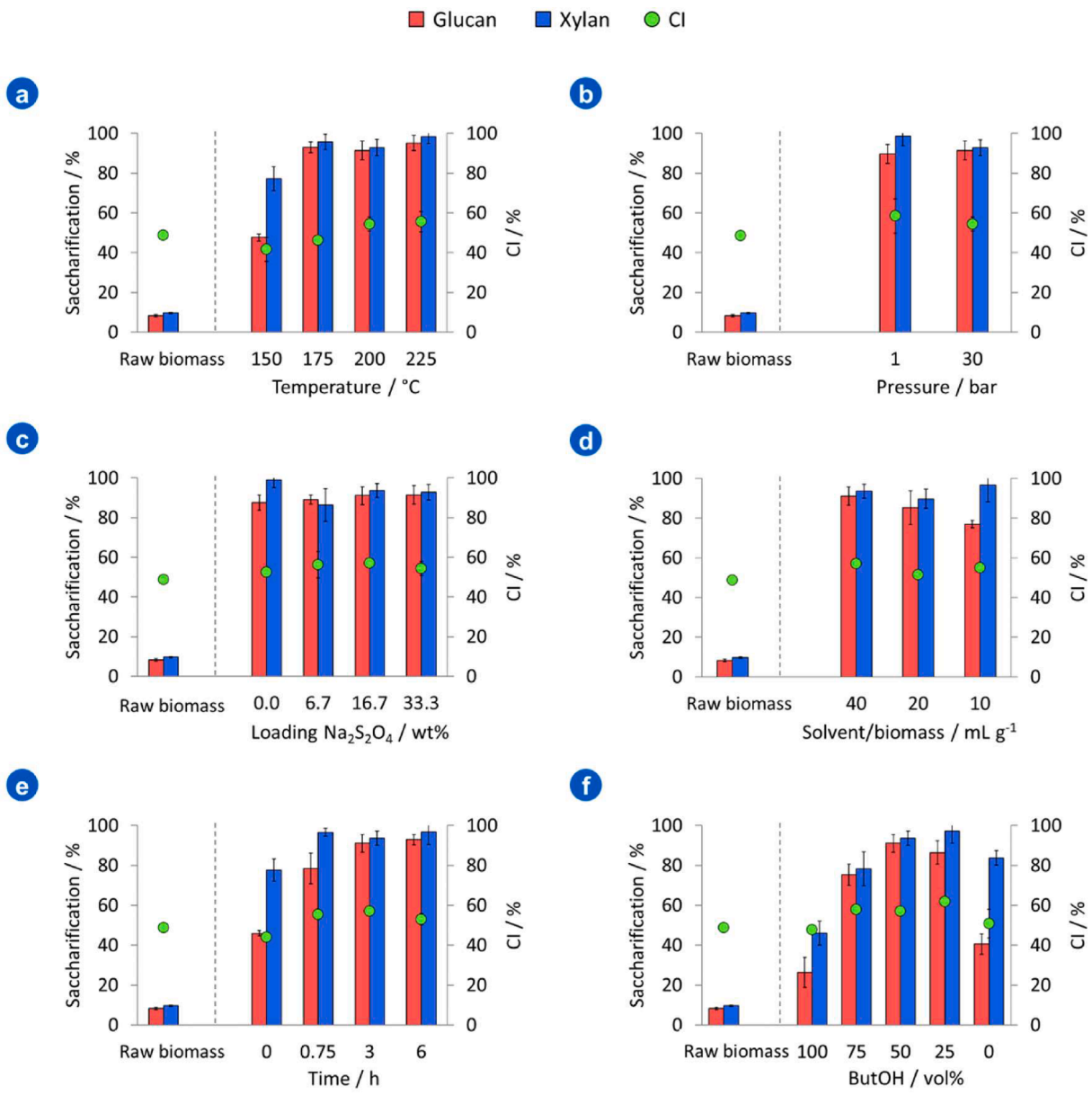


Fig. 3. Yields of saccharification of glucan and xylan (red and blue bars) and cellulose crystallinity index (green circles) of the solid fractions obtained from the DAOF of birch sawdust carried out at different operating temperatures (a), exogenous pressures (b), loadings of $Na_2S_2O_4$ (c), solvent/biomass ratios (d), reaction times (e), and *n*-butanol/water ratios (f). Unless otherwise specified, fractionation experiments were performed treating 3 g of birch sawdust in 120 mL of an equivolumetric mixture of *n*-butanol and water, at 200 °C, under 30 bar of N_2 (introduced at ambient temperature), in the presence of $Na_2S_2O_4$ (33.3 % w/$w_{biomass}$ for panels a and b; 16.7 % w/$w_{biomass}$ for panels d–f), for a duration of 3 h. (For interpretation of the references to colour in this figure legend, the reader is referred to the web version of this article.)

solvent resulted in the complete disappearance of the bands at 1235 cm^{-1}, and 1510 cm^{-1}, as well as in a substantial reduction of the bands at 1465 cm^{-1} and 1595 cm^{-1}, pointing out a more extensive removal of hemicellulose and lignin [52,53]. The use of water alone resulted in more apparent bands corresponding to lignin (1045, 1465, 1510 and 1595 cm^{-1}) [52–54], highlighting its worse solubilization or its increased redeposition on the pulp surface. In addition, the presence of a more evident band at 1098 cm^{-1} indicated a higher content of crystalline cellulose [53]. Consistent with the improved removal of amorphous components, the CIs determined for the pulps obtained from processing with mixtures of *n*-butanol and water were found to be greater than those measured for the pure solvents (Fig. 3f). Further inspection of the solid fractions *via* SEM revealed that a treatment in *n*-butanol caused a smoothening of the pulp surface and exposed tightly packed bundles of fibers, which were partially disassembled upon the addition of water to the mixture (Fig. S8a–c). On the contrary, the use of water alone led to an extensive fragmentation of lignocellulose and a consequent redeposition of the debris on the fibers, which were completely covered (Fig. S8d). In line with this, a higher digestibility of the preserved polysaccharides was measured when *n*-butanol and water were employed together, with the highest yield of glucan saccharification of 91 % determined for an equivolumetric mixture of the two solvents (Fig. 3f).

3.4. Organic fraction: Lignin oil

The solubilized lignin was isolated from the organic liquid fractions *via* solvent evaporation followed by liquid–liquid extraction with dichloromethane and water, according to a procedure reported elsewhere [28,61]. Evaporating the solvent from the dichloromethane

extracts yielded viscous brown lignin oils, comprising lignin derivatives and humic products [32] The molecular weight distribution (MWD) of the components of lignin oils and the phenolic monomers composition of the oils were determined *via* GPC and *via* GC–MS/FID, respectively.

In line with previous reports on organosolv and RCF processes [62,63], lignin solvolysis and the yield of lignin oil were found to increase substantially with temperature (Table 1, entries 1–5). A major increment of the yield of lignin oil from 4 wt% to 63 wt% of acid insoluble lignin in the initial biomass was measured between 150 and 175 °C, pointing to a threshold temperature for achieving an effective solvolytic disassembly of lignin-carbohydrate linkages. Yields of oil greater than 100 wt% were observed at high temperatures (greater than200 °C), highlighting the incorporation of humins in the oil, most probably generated upon the extensive decomposition of C5 and C6 polysaccharides achieved under these conditions [49,64,65]. GPC analyses of the lignin oils extracted at different temperatures are shown in Fig. 4a. As the temperature was raised from 150 to 200 °C, a peak at about 150 g mol^{-1} appeared and became preponderant, indicating the enhanced formation of phenolic monomers. Further increase of the temperature resulted in a gradual disappearance of the monomers peak in favor of the formation of larger fragments, suggesting the occurrence of repolymerization reactions. Concomitantly, the formation of small fragments (MW < 100 g mol^{-1}) was observed, possibly corresponding to dealkylated monophenolics or carbohydrate derivatives (*e.g.* furans). Overall, the estimation of the weight average molecular weight (M_W) of lignin oils (Table S4, entries 1–5) clearly showed that M_W diminished as the operating temperature increased, with the highest drop of M_W, from about 1800 to 1000 g mol^{-1}, that was determined for the range

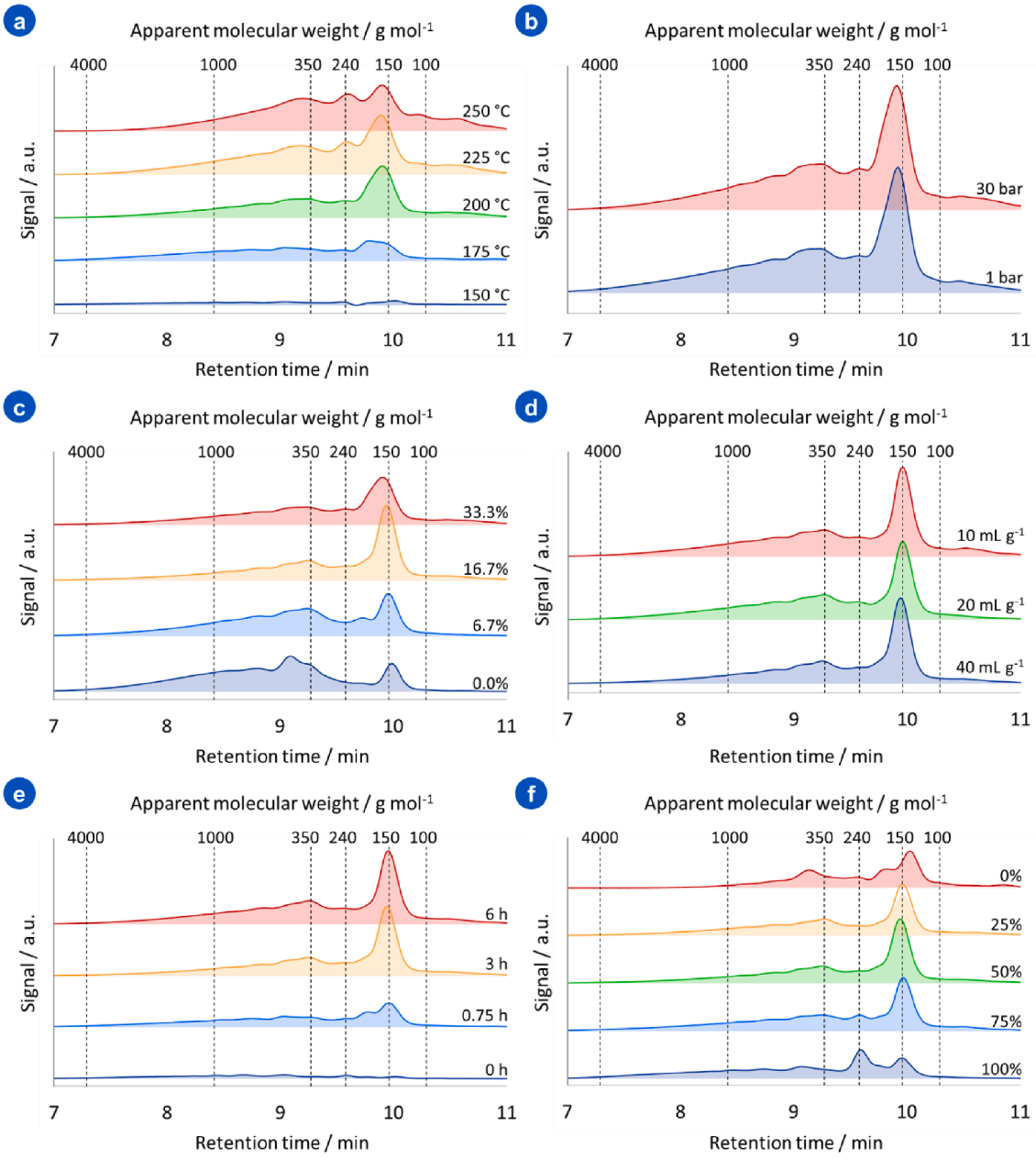


Fig. 4. GPC chromatograms showing the molecular weight distribution of the components of lignin oils obtained from the DAOF of birch sawdust carried out at different operating temperatures (a), exogenous pressures (b), loadings of $Na_2S_2O_4$ (c), solvent/biomass ratios (d), reaction times (e), and *n*-butanol/water ratios (f). Unless otherwise specified, fractionation experiments were performed treating 3 g of birch sawdust in 120 mL of an equivolumetric mixture of *n*-butanol and water, at 200 °C, under 30 bar of N_2 (introduced at ambient temperature), in the presence of $Na_2S_2O_4$ (33.3 % w/$w_{biomass}$ for panels a and b; 16.7 % w/$w_{biomass}$ for panels d–f), for a duration of 3 h. The area underneath each chromatogram was normalized with respect to the yield of lignin oil obtained for the corresponding experiment.

175–200 °C, corresponding to extensive formation of monophenolics. Consistently, GC–MS/FID analyses of the lignin oils revealed that the monomer yield increased with temperature, from 1.2 wt% of acid insoluble lignin in the initial biomass at 150 °C up to 18.1 wt% at 200 °C, then diminished as the temperature was raised further (Fig. 5a and Table S5). A broad variety of monomeric compounds was observed, including species with side chains containing carbonyl groups (**1**–**4**), species with 4-propenyl or 4-propyl side chains (**5** and **6**, respectively), and species missing a side chain (**7**). Such a broad spectrum of products can be explained by the combination of acid-catalyzed and reductive pathways for the cleavage of β-O-4 linkages in lignin [32]. Raising the operating temperature above 200 °C resulted in the gradual depletion of **1**–**4**, likely due to dealkylation and repolymerization reactions, as evidenced by the increased yield of **7** and by the presence of peaks at higher molecular weights observed in the GPC profiles. On the other hand, the consumption of **5** appeared to be accompanied by the formation of **6**, suggesting – as demonstrated with model compounds [32] – the ability of dithionite to promote the hydrogenation of C=C bonds in the side chains of lignin moieties at high temperature.

The nitrogen pressure was found to have virtually no influence on the yield of lignin oil and on the MWD of the components of lignin oil (Table 1, entries 3, 6; Fig. 4b and Table S4, entries 3, 6), as well as on the distribution of monophenolic products (Fig. 5b and Table S6), confirming that effective valorization of lignin to monoaromatics could be achieved in the absence of external pressurization, thereby advantageously relaxing the equipment requirement to withstand elevated pressure (see below).

The loading of sodium dithionite did not appear to affect the yield of lignin oil, which remained around 90–95 wt% (Table 1, entries 3, 7–9). On the contrary, the dithionite loading was found to exert a major impact on lignin depolymerization (Fig. 4c and Table S4, entries 3, 7–9). The GPC profiles in Fig. 4c show that the introduction of dithionite

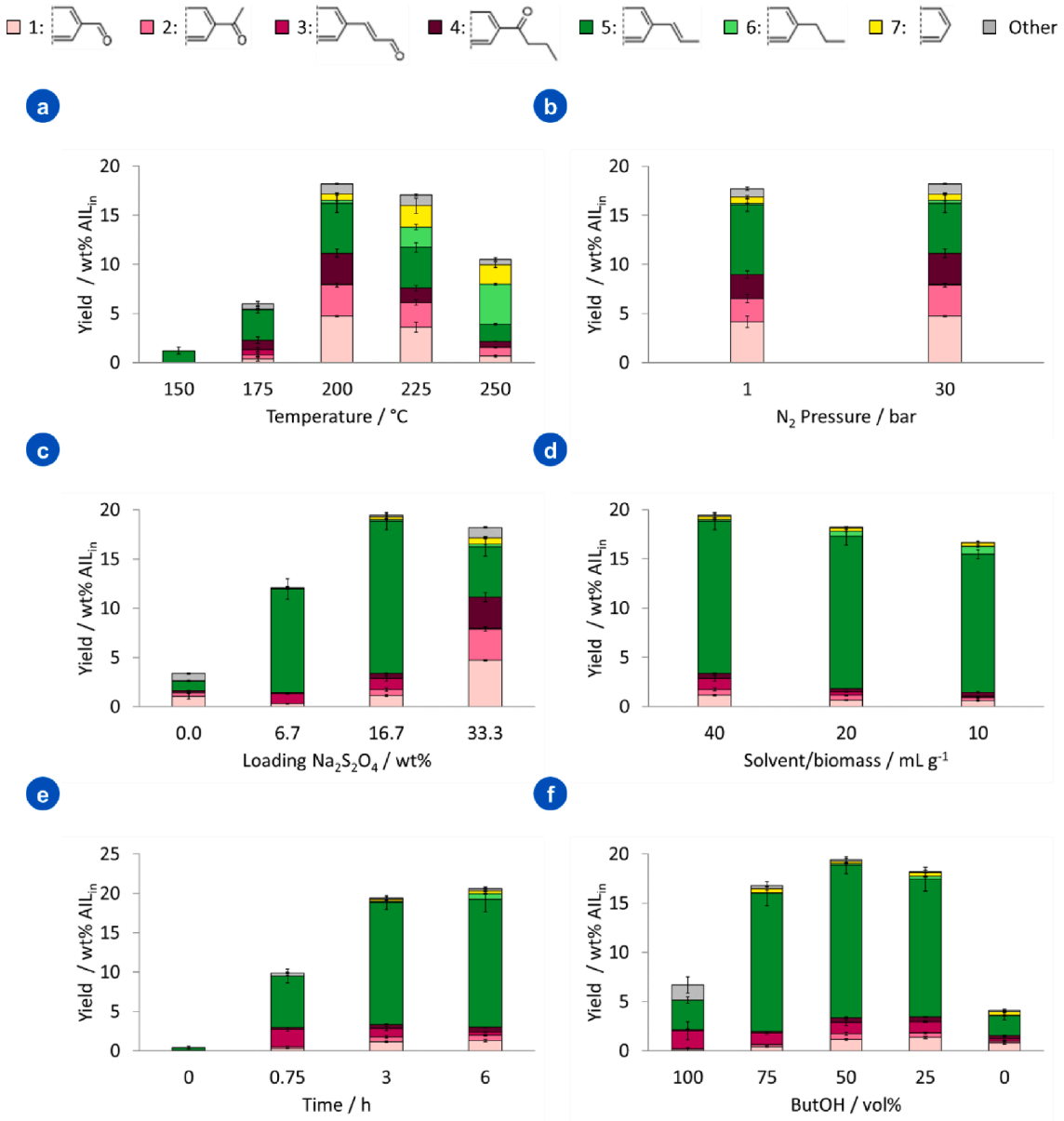


Fig. 5. Yield of phenolic monomers as determined by GC analysis of the lignin oils obtained from the DAOF of birch sawdust carried out at different operating temperatures (a), exogenous N_2 pressures (b), loadings of $Na_2S_2O_4$ (c), solvent/biomass ratios (d), reaction times (e), and *n*-butanol/water ratios (f). Unless otherwise specified, fractionation experiments were performed treating 3 g of birch sawdust in 120 mL of an equivolumetric mixture of *n*-butanol and water, at 200 °C, under 30 bar of N_2 (introduced at ambient temperature), in the presence of $Na_2S_2O_4$ (33.3 % w/$w_{biomass}$ for panels a and b; 16.7 % w/$w_{biomass}$ for panels d–f), for a duration of 3 h. The monomer yield was calculated with respect to the acid insoluble lignin (AIL) content in the initial biomass.

within the fractionation process led to a considerable boost of the phenolic monomers fraction, accompanied by a gradual flattening of the tail extending to high molecular weights, which confirms the essential role of dithionite with respect to enhancing lignin depolymerization and partially preventing its recondensation. Importantly, the adoption of a dithionite loading of 16.7 % w/$w_{biomass}$ led to a monomers peak in the chromatogram comparable to that observed for a loading of 33.3 % w/$w_{biomass}$, as well as to a similar M_W, suggesting that the amount of dithionite fed to the process could be advantageously reduced, compared to what was reported in a previous study on the DAOF [32]. The effective production of monophenolics was confirmed by GC analyses of the lignin oils, which showed that the highest yield of 19.4 wt% was attained at a loading of 16.7 % w/$w_{biomass}$ (Fig. 5c, Table S7). Most strikingly, the loading of reducing agent was found to remarkably affect the monophenolics composition (Fig. 5c, Table S7). In the absence of dithionite, a low yield of monomers of 3.6 wt% was obtained, mainly comprising **1**, **2**, and **5**. The use of a dithionite loading of 6.7 % w/$w_{biomass}$ resulted in a substantial increase in the formation of **5** (with a yield of 10.5 wt%), highlighting an enhanced reductive cleavage of inter-unit linkages in lignin structures in the presence of the reducing agent [32]. Further increase of the dithionite loading to 16.7 % w/$w_{biomass}$ boosted the yield of **5** up to 15.5 wt%, and also led to a slightly larger formation of species with side chains containing carbonyl groups (**1**–**4**). Surprisingly, the use of a higher loading of 33.3 % w/$w_{biomass}$ resulted in a diminution of the yield of **5** (down to 5.1 wt%) and in larger yields of **1**, **2**, and **4**, possibly indicating a worse performance of dithionite with respect to the reductive cleavage of lignin in this scenario. A tentative explanation for such behavior could be found in the tendency of the reducing agent to undergo auto-catalytic decomposition in acidic aqueous media [66,67].

The yield of lignin oil increased from 93 wt% to 119 wt% when the solvent/biomass ratio was decreased from 40 to 10 mL g^{-1} (Table 1, entries 9–11), pointing to a larger incorporation of humins in the oil, in agreement with the lower recoveries of C5 and C6 polysaccharides discussed above. The MWD of the components of the lignin oils showed a considerable formation of monophenols at all solvent/biomass ratios (Fig. 4d and Table S4, entries 9–11), with a slightly more apparent tailing in the GPC profiles observed at lower ratios, suggesting incomplete lignin depolymerization or enhanced repolymerization. Further inspection by GC analysis revealed a slight decline of the overall yield of monomers with decreasing solvent/biomass ratio (Fig. 5d and Table S8), and a rather uniform diminution of the yield of **1**–**5**, possibly due to their participation in recondensation reactions. Concomitantly, **6** was formed, highlighting the partial hydrogenation of unsaturated side chains in lignin moieties, achieved as a result of the larger concentration of dithionite in the medium.

Longer reaction times resulted in larger yields of lignin oil, corresponding to the progressive solubilization of lignin (Table 1, entries 9, 12–14). A yield of 115 wt% was obtained after 6 h, indicating the incorporation of humic products in the oil. The MWD of the components of the oil was also affected by the processing time (Fig. 4e and Table S4, entries 9, 12–14), with the appearance of a monomers peak in the GPC profile at 0.75 h that increased at longer times. A tail extending to higher molecular weights was observed that gradually became more evident with time, suggesting partial repolymerization or the extraction of larger lignin fragments from the lignocellulose matrix [68]. GC analysis corroborated GPC results, showing that moderate production of monophenolics was achieved at 0.75 h, with a yield of monomers of 9.9 wt% and a prominent formation of **5** (yield of 6.5 wt%) and **3** (yield of 1.6 wt%) (Fig. 5e and Table S9). Longer reaction times led to an increase of the yield of monomers up to 20.6 wt% after 6 h, with a boost of the yield of **5** (up to 16.2 wt%) and a diminution of the yield of **3** (down to 0.3 wt%), possibly due to repolymerization reactions. The formation of monophenolics with shorter or missing side chains (**1**, **2**, **7**) was detected at longer times, indicating the occurrence of dealkylation reactions. The marginal production of **6** pinpoints the partial hydrogenation of lignin moieties under the action of dithionite.

Processing lignocellulosic biomass in pure *n*-butanol and pure water led to lignin oil yields of 63 wt% and 44 wt%, respectively (Table 1, entries 9, 15–18). On the other hand, the combined use of the two solvents resulted in substantially larger oil yields (up to 96 wt%), clearly highlighting the superior performance of the mixture for the extraction of lignin. GPC analyses of the lignin oils showed that the adoption of *n*-butanol alone yielded a lignin oil with the highest M_W of ~ 1800 g mol^{-1}, due to the poor disassembly of the extracted lignin and the high solubility of large lignin fragments in *n*-butanol. On the contrary, the use of water alone led to the lowest M_W of ~ 450 g mol^{-1} (Table S4 entries 9, 15–18). The latter observation is chiefly due to the low solubility of larger fragments in water, rather than to a more extensive depolymerization of lignin, as illustrated by the relatively flat GPC profile at high molecular weights, and by the small peak corresponding to lignin monomers (Fig. 4f). Indeed, the best conditions for lignin depolymerization coincided with the use of a mixture of the two solvents, which led to a marked boost of the peak for monophenolics, up to a maximum achieved for the case of an equivolumetric mixture. Further inspection of the yield of lignin monomers *via* GC confirmed the conclusions made based on GPC (Fig. 5f and Table S10). The yield of monophenolics was substantially increased by the combined use of *n*-butanol and water, up to a maximum of 19.4 wt%, achieved for an equivolumetric mixture. A relevant finding is that a high yield of monophenolics of 18.2 wt% could also be attained in the presence of a low fraction of *n*-butanol (25 vol%), suggesting that the amount of *n*-butanol co-solvent used for the fractionation could be conveniently diminished without considerably affecting the production of monoaromatics.

With the goal of gaining further insight into the structural features of the aromatic species produced during the DAOF, samples of lignin oil were subjected to ^{1}H–^{13}C HSQC NMR analysis. In particular, samples obtained in the presence of different loadings of dithionite were analyzed, to investigate the role of the reducing agent with respect to the formation of defined structural patterns (Table S11). In agreement with the previously discussed GC results, Figs. S9–S12 and the data reported in Table S12 clearly show that the use of a dithionite loading of 16.7 % w/$w_{biomass}$ boosted the formation of species possessing 4-propenyl side chains compared to a treatment carried out in the absence of dithionite. At the same time, a slightly larger formation of 4- propenal end-units and other structural motifs containing carbonyl groups in their side chains (*e.g.* acetosyringone, acetoguaiacone, etc.) was observed. Further increase of the loading of reducing agent led to a sharp diminution of the signals corresponding to 4-propenyl and 4-propenal end-units and a remarkable increment of those corresponding to syringaldehyde, acetosyringone and acetoguaiacone structural motifs. These results confirm that the adoption of a dithionite loading of 16.7 % w/$w_{biomass}$ is optimal for enhancing the reductive cleavage of β-O-4 linkages in lignin during the DAOF. Interestingly, the formation of 4-propyl and 4-propanol end-units was determined in the presence of dithionite, pointing out its ability to reduce C═C bonds in the side chains of lignin moieties formed upon reductive cleavage of β-O-4 bonds [32]. Lignin inter-unit linkages were also found to be affected by the loading of the reducing agent. Notably, the cross signals corresponding to β-O-4 bonds gradually disappeared at higher dithionite loadings, in line with the trend observed in a previous study with lignin model compounds [32]. Similarly, the signals corresponding to other native lignin linkages such as β-β resinol and β-5 phenylcoumaran were found to decrease at higher dithionite loadings, likely due to the cleavage of labile ether bonds in these structures [14]. In the absence of dithionite, a low portion (~25 %, based on total aromatic units) of the ^{13}C–^{1}H HSQC spectrum could be assigned to known structural motifs (Table S12). The unassigned portion of the spectrum may be associated with the formation of non-native C—C linkages between lignin units, resulting from repolymerization reactions [69]. Remarkably, in the presence of dithionite, the unassigned portion of the spectrum was lower compared to that determined in the absence of the reducing agent, suggesting that dithionite can

partially prevent lignin recondensation, in line with the lower amount of high-MW fragments and of the higher yields of monophenolics observed *via* GPC and GC analysis. Overall, NMR analysis showed that the dithionite loading has a marked impact on the end-units and inter-unit linkages in lignin derivatives (which will ultimately affect the physico-chemical properties of lignin oil).

3.5. Aqueous fraction: non-condensed carbohydrate derivatives

Even though the aqueous liquid fraction is ultimately considered as wastewater in the process, it was analyzed with the goal of gaining a more complete insight in the fate of biomass and dithionite derivatives during the DAOF. Thus, the aqueous liquid fractions obtained from the DAOF were subjected to pH measurement and HPLC analysis to determine the influence of different process configurations on the acidity of the medium and on the production of xylose, 1,2-propylene glycol and formic acid, which were recognized as the major non-condensed carbohydrate derivatives formed during the DAOF [32].

As a general trend, rather low yields of carbohydrate derivatives were measured for the different process configurations that were explored (Table 1). Consistently with this observation, the intermediates formed during (hemi)cellulose solvolysis were reported to be more prone to undergo degradation/recondensation compared to lignin derivatives [70]. Yet, all the studied process variables (except nitrogen pressure–Fig. S13b and Fig. S14b) were found to affect the acidity of the medium and the formation of non-condensed carbohydrate derivatives.

A treatment temperature of 150 °C led to a low pH of 3.4 and to the formation of acetic acid, most probably resulting from deacetylation of hemicellulose [71]. The pH increased sharply at 175 °C, then remained around pH 6 at higher temperatures (Fig. S13a). This behavior may be due to the partial decomposition of dithionite, as previously reported by other authors [66]. On the other hand, almost no production of carbohydrate derivatives was measured at 150 °C (Fig. S14a). Such observation can be explained by the little solvolysis of (hemi)cellulose occurring under these conditions (see above). The yield of 1,2-propylene glycol and formic acid increased consistently up to 1.2 wt% and 6.3 wt% of polysaccharides in the initial biomass, respectively, at 200 °C, pointing to an enhancement of carbohydrate decomposition [37,38]. Further rise of the operating temperature caused a diminution of the yield of formic acid, possibly due to its conversion toward gaseous products [37].

Higher loadings of dithionite led to an increase of the pH despite the presence of larger concentrations of formic and acetic acid in the medium (Fig. S13c), suggesting an increment of dithionite decomposition [66,67]. The gradual decline of the yield of xylose and the concomitant boost of the yield of formic acid at increasing dithionite loadings, indicate that dithionite promotes carbohydrate decomposition during the DAOF, with a total yield of non-condensed carbohydrate derivatives that increased with the loading of the reducing agent from 3.4 wt% in the absence of dithionite to 7.5 wt% at a loading of 33 % $w/w_{biomass}$ (Fig. S14c). An analogous behavior was observed for experiments carried out at different solvent/biomass ratios. The pH remained stable at 4.7 even though the concentrations of formic and acetic acid increased with decreasing solvent/biomass ratios (Fig. S13d). In addition, Fig. S14d shows a buildup of the yield of formic acid at the expense of xylose at lower solvent/biomass ratios (*i.e.* higher dithionite concentration in the medium). Similarly to the action of bisulfite ions during acid sulfite pulping [72,73], dithionite could contribute to carbohydrate degradation by reacting with sugars to yield organic acids. Formic acid may be formed *via* further fragmentation reactions [74].

Halting the fractionation immediately after reaching the setpoint temperature (*i.e.* "0 h" experiment) resulted in the formation of acetic acid and in a low pH of the medium of 4.1 (Fig. S13e). At longer reaction times, the pH rose up to 4.7 in view of the action of dithionite [66]. Consistently with the high recoveries of C5 and C6 polysaccharides determined in the solid fraction, a minimal formation of carbohydrate derivatives was determined at a short reaction time (Fig. S14e). Conversely, longer durations resulted in the increase of the yields of xylose, 1,2-propylene glycol, and formic acid, by virtue of a more extensive solvolysis of (hemi)cellulose.

The decrease of the *n*-butanol/water ratio led to a decline of the pH of the medium from 4.7 at 75 vol% *n*-butanol, to 3.9 in pure water, possibly due to a more effective deacetylation of hemicellulose (Fig. S13f). The presence of *n*-butanol in the solvent mixture appeared to favor the production of formic acid, which reached a maximum of 2.8 wt % for a mixture containing 75 vol% *n*-butanol. On the contrary, the use of greater amounts of water led to a decrease of the yield of formic acid, and a gradually larger yield of xylose (Fig. S14f), pointing to the crucial role of solvent composition with respect to the fate of solubilized carbohydrates during the DAOF.

3.6. Economic feasibility of the DAOF

A techno-economic assessment (TEA) was conducted to study the economic feasibility of the DAOF process. From the process flow diagram (Fig. 6) three product streams of interest were identified: a cellulosic pulp, a monophenolics-rich stream (cyclohexane oil, obtained after the extraction of monophenolics with cyclohexane–see Supporting Information), and an oligophenolics-rich stream (residue obtained after the extraction of monophenolics). The aqueous stream was considered as wastewater. The TEA presented by Tschulkow *et al.* for reductive catalytic fractionation (RCF) was used as a starting point for the present assessment [75]. As many similarities exist between the DAOF and RCF processes with respect to unit operations and plant sections needed, the CAPEX scale-up was assumed to be the same for RCF and DAOF (Fig. S15). This assumption makes the present TEA more conservative since the DAOF does not rely on the use of heterogeneous catalysts or hydrogen gas, and lower temperatures and pressures are adopted, resulting in less stringent safety requirements and, overall, in a less costly reactor design. Moreover, it was assumed that the efficiency of the solvent recovery steps within the DAOF was equal to that reported for the RCF [11,75].

As the DAOF process is still at the *proof-of-concept* stage (technology readiness level (TRL) of 3–4), a higher discount rate of 17.5 % was considered for the DAOF, versus 15 % for the more mature RCF (TRL 4–5). A project lifetime of 20 years was fixed, with an annual operating time of 8000 h. Based on these hypotheses and assuming that the experimental data discussed in the previous sections were scalable, the net present value (NPV) for the DAOF configuration corresponding to Table 1, entry 9, which led to the maximum yield of monophenolics, was calculated. Considering a base case annual dry birch wood intake of 1500 kt y^{-1} and the assumptions reported in Table S13 and Table S14 for the process operative expenditure (OPEX) and revenues, such DAOF configuration has a NPV of 37 M€. This result suggests that the DAOF configuration would be economically feasible in wood abundant regions (such as North America and Northern European countries), where the feedstock intake of the biorefinery could be conveniently met. Importantly, the present analysis was based on a relatively conservative birch wood cost of 171 € t^{-1}. In other works, lower costs were reported (down to ~ 80 € t^{-1}) [11,76,77]. Hence, the impact of the feedstock cost on the NPV of the DAOF process was assessed by performing a sensitivity analysis (Fig. S16). A substantial increase of the NPV for the base case scenario was determined at decreasing feedstock cost, up to a NPV of 910 M€ attained for a feedstock cost of 80 € t^{-1}, hinting at an even higher economic potential of the DAOF in wood-abundant regions, where the feedstock cost may very well be lower than that initially assumed in the present assessment.

Considering the dependence of the NPV on the feedstock capacity level, the break-even point (at which the NPV equals zero) is reached at a capacity level of 1350 kt y^{-1} (Fig. S17). Thus, in less wood-abundant regions, efforts will be required to make the DAOF process more feasible at lower annual feedstock intakes. From this point of view, it is interesting to inspect the influence of variations of the OPEX and of the

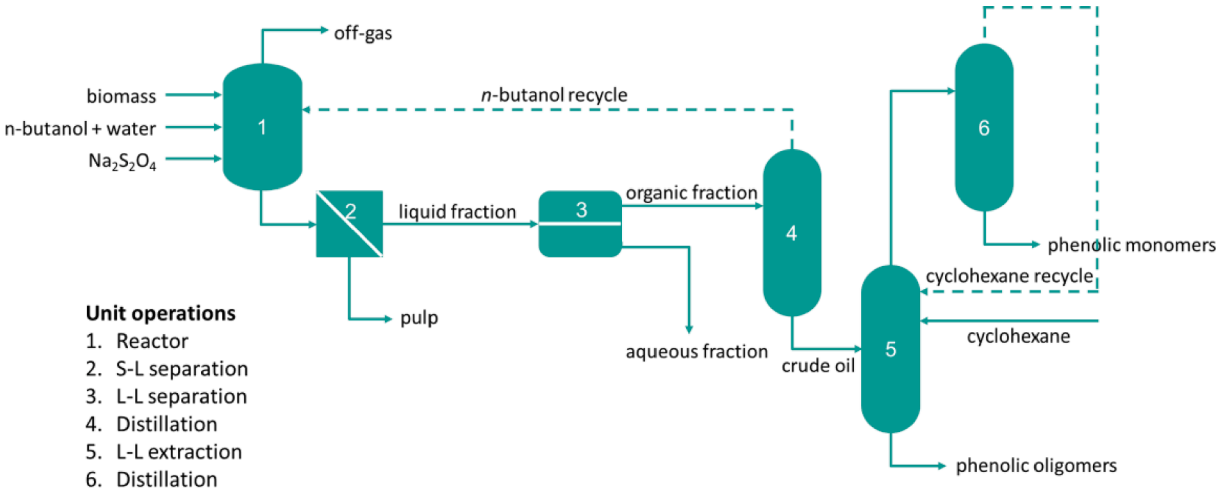


Fig. 6. Flow diagram depicting the basic unit operations for the DAOF process. Streams for solvents recycle are indicated with dashed lines.

product revenues on the NPV of the DAOF.

Table S13 shows that the cost of sodium dithionite contributes to a large fraction of the OPEX, suggesting that the use of lower amounts of dithionite could be more favorable. Thus, the influence of the loading of dithionite on the NPV of the DAOF was evaluated, according to the experimental configurations reported in Table 1, entries 3, 7–9. The yields of pulp, phenolic monomers and oligomers for these configurations are summarized in Table S15. In view of the extensive variability of the market price for monophenolics reported in the literature (~1750–~12000 € t^{-1}) [61,75,78], a conservative price range from 1500 to 6500 € t^{-1} was considered for this study. The outcomes of the analysis are reported in Table 2. Herein, three different regions can be distinguished: (i) for monomers selling prices between 1500 € t^{-1} and 5000 € t^{-1} a *blank* organosolv process (performed in the absence of dithionite) would be the most convenient, (ii) for a price of 5500 € t^{-1} the process configuration with a dithionite loading of 6.7 % $w/w_{biomass}$ would be the most favorable, and (iii) for a price equal or greater than 6000 € t^{-1} the configuration with a dithionite loading of 16.7 % $w/w_{biomass}$ would be the most promising.

Besides the cost of dithionite, that of *n*-butanol represented a considerable expenditure as well (Table S13), and the use of lower amounts of *n*-butanol could be more favorable. Therefore, a second sensitivity analysis was carried out to evaluate the effect of the *n*-butanol/water ratio on the NPV of the DAOF, according to the experimental results reported in Table 1, entries 9, 15–18. The yields of pulp, phenolic monomers and oligomers for these configurations are summarized in Table S16. The outcomes of such analysis are illustrated in Table 3. As a result of the low amount of monophenolics produced in the presence of the pure solvents, neither the use of *n*-butanol or water alone led to economically feasible configurations. On the other hand, for monomers selling prices equal to or greater than 2000 € t^{-1}, the DAOF configurations with 25 vol% and 50 vol% *n*-butanol were found to be feasible (the configuration with 75 vol% *n*-butanol was also found to be feasible for monomer prices equal or greater than 2500 € t^{-1}), with the use of an equivolumetric mixture of *n*-butanol and water resulting in the largest NPVs.

Overall, despite the conservative hypotheses that were made in terms of CAPEX, this TEA shows that the DAOF can be economically viable. In this respect, the loading of dithionite and the *n*-butanol/water ratio applied were highlighted to have a decisive influence on the process profitability, and the DAOF configuration employing a dithionite loading of 16.7 % $w/w_{biomass}$ and an equivolumetric mixture of *n*-butanol and water appeared to be the most promising. Notably, the economic potential of the DAOF was shown to be ultimately dependent on the selling price for phenolic monomers.

Future work should focus on reducing the OPEX further to improve the economic feasibility of the DAOF. The recovery of dithionite derivatives downstream and the regeneration of the reducing agent could be explored. In addition, the replacement of *n*-butanol with less expensive alcohols (*e.g.* methanol, ethanol) could contribute to diminish the operating costs.

Table 2
NPVs calculated for DAOF configurations using different dithionite loadings.

Monomers price (€ t^{-1})	NPV (M€)[a] $Na_2S_2O_4$ loading (wt%)[b] 0.0	6.7	16.7	33.3
1500	995	473	−46	−955
2000	1026	577	120	−801
2500	1057	680	285	−646
3000	1087	784	451	−491
3500	1118	887	617	−336
4000	1149	991	782	−182
4500	1179	1094	948	−27
5000	1210	1197	1114	128
5500	1241	1301	1279	283
6000	1272	1404	1445	437
6500	1302	1508	1611	592

[a] Calculated for a birch feedstock capacity level of 150 kt y^{-1}. [b] Expressed with respect to the weight of biomass.

Table 3
NPVs calculated for DAOF configurations using different *n*-butanol/water ratios.

Monomers price (€ t^{-1})	NPV (M€)[a] *n*-butanol/water (%vol ButOH) 100	75	50	25	0
1500	−797	−233	−46	−35	−638
2000	−740	−89	120	120	−603
2500	−684	54	285	276	−568
3000	−628	198	451	431	−533
3500	−571	341	617	587	−498
4000	−515	485	782	742	−463
4500	−459	628	948	898	−428
5000	−402	772	1114	1053	−393
5500	−346	915	1279	1208	−358
6000	−290	1058	1445	1364	−323
6500	−233	1202	1611	1519	−288

[a] Calculated for a birch feedstock capacity level of 150 kt y^{-1}.

3.7. DAOF of different lignocellulosic feedstocks

In In order to explore the process robustness with respect to the treatment of lignocellulose from different sources, two herbaceous

biomasses–miscanthus grass (*Miscanthus* × *giganteus*) and wheat straw (*Triticum aestivum*)–as well as a softwood (Norway spruce, *Picea abies*), were subjected to DAOF according to the conditions reported in Table 1, entry 9. The outcomes of the fractionation were compared to those observed for the treatment of birch sawdust. All biomasses possessed a particle size ≤ 2 mm [34]. Their composition is reported in Table S1. Table S17 shows that the highest recovery of OM in the pulp were obtained for the treatment of miscanthus (52 wt% of OM in the initial biomass) and spruce wood (54 wt%), in view of the large cellulose content of these feedstocks. Birch wood led to the highest recovery of OM in the organic fraction (26 wt%), likely due to a more facile lignin solvolysis for the case of hardwoods compared to softwoods and herbaceous biomass [79]. The greatest recovery of OM in the aqueous fraction was obtained for the processing of wheat straw (15 wt%), probably determined by the high content of water-soluble extractives in this biomass. Overall, a mass balance comprised between 78 wt% (for birch wood) and 85 wt% (for spruce wood) was obtained, highlighting that a partial conversion of biomass to volatiles occurred for all scenarios.

The properties of the different product streams obtained after the DAOF of each feedstock are summarized in Table 4. Large recoveries of C6 polysaccharides in the pulp (≥90 wt%) were determined for all scenarios, indicating excellent cellulose preservation. At the same time, hemicellulose was extensively solubilized, with a removal greater than 70 wt%. A relatively low delignification was achieved for the treatment of spruce wood. A similar outcome was reported also for the organosolv and the RCF treatment of softwoods [48,61], and the minor delignification was associated with the chemical structure of lignin that features a lower content of cleavable β-O-4 linkages, and a greater content of guaiacyl-units, possessing a higher tendency to undergo condensation reactions [2,61,79]. Another explanation for this behavior could be found in the generally less porous morphology of softwood biomass compared to hardwood and herbaceous feedstocks [15,80] which may determine a higher mass transfer resistance for the solvolytic extraction of lignin [34]. These findings were supported by further FTIR analyses of the solid fractions (Fig. S18), which exhibited more apparent bands at 1160 cm^{-1} and the disappearance of the band at 1740 cm^{-1} for all biomasses, corresponding to a larger cellulose content and to the partial removal of hemicellulose and lignin, respectively. In addition, the bands at 1235 cm^{-1} and 1510 cm^{-1} (associated with hemicellulose and lignin) were found to vanish after treatment, and the band at 1595 cm^{-1} (associated with lignin) decreased for all feedstocks except spruce wood, confirming the less effective removal of lignin for softwood biomass. In line with these observations, the enzymatic convertibility of the isolated polysaccharides was considerably smaller for spruce wood compared to the other feedstocks, whose treatment led to highly digestible pulps (with yields of saccharification ≥ 90 %). On the other hand, the partial removal of amorphous components during the DAOF resulted in a slight increase of the CI of the solid fractions for all biomass types (Table 4, Fig. S19).

In agreement with the lower delignification observed for spruce wood, the yield of lignin oil isolated from the organic fraction was modest for the treatment of this biomass (Table 4). The GPC profiles of the lignin oils obtained from the treatment of the various feedstocks were different from one another (Fig. 7a). A peak for monophenolics was observed in all cases, which became larger in the order: spruce wood < wheat straw < miscanthus < birch wood. A higher abundance of high MW fragments was found for the treatment of wheat straw, as indicated by the more prominent peak at 350 g mol^{-1} and by the presence of an additional peak at 520 g mol^{-1}, as well as by the thick tail extending to higher molecular weights. These results suggest that a more effective depolymerization of lignin could be achieved when the DAOF was applied to birch sawdust.

Further inspection of the lignin oils *via* GC analysis corroborated the previous observations, with the greatest yield of monomers obtained for birch wood (19.4 wt% of acid insoluble lignin in the initial biomass), followed by miscanthus (13.1 wt%), wheat straw (11.6 wt%) and spruce wood (7.3 wt%) (Fig. 7b, Table 4). Remarkably, Fig. 7b and Table S18 show that, despite some variability in the yields of species with side chains containing carbonyl groups, a relatively high yield of monophenolics with 4-propenyl side chains was attained for all types of biomasses employed, confirming that the DAOF selectively promoted the reductive depolymerization of lignin from the various feedstocks.

A generally low yield of non-condensed carbohydrate derivatives was observed for the treatment of the different biomasses (Fig. S20), with a marginal release of xylose and the formation of low amounts of 1,2-propylene glycol and formic acid, confirming that the intermediates generated upon (hemi)cellulose decomposition are not promptly stabilized against recondensation during the DAOF, regardless of the biomass source.

Overall, while all the explored lignocellulosic feedstocks were found to be suitable for the DAOF, hardwood and herbaceous biomass appeared to be particularly prone to be valorized with this approach.

Table 4
Biomass derivatives obtained for the DAOF of different lignocellulosic feedstocks.

			Biomass[a]			
			Birch	Miscanthus	Wheat straw	Spruce
Solid fraction	Recovery (wt%)	C5[b]	20 ± 2	24 ± 3	25 ± 2	30 ± 3
		C6[b]	92 ± 2	96 ± 2	95 ± 3	94 ± 2
		Lignin[c]	27 ± 3	29 ± 3	36 ± 4	44 ± 2
	Saccharification[d] (%)	Glucan	91 ± 5	92 ± 5	87 ± 7	38 ± 7
		Xylan	94 ± 4	95 ± 4	89 ± 10	46 ± 2
	CI[e](%)		57 ± 1	70 ± 3	70 ± 2	69 ± 4
Organic fraction	Yield (wt%)	Lignin oil[c]	93 ± 6	86 ± 1	94 ± 6	65 ± 2
		Monophenolics[c]	19.4 ± 1.8	13.1 ± 2.2	11.6 ± 1.6	7.3 ± 0.3
Aqueous fraction	Yield (wt%)	C5, C6 derivatives[f]	4.0 ± 0.4	3.1 ± 0.1	4.1 ± 0.5	3.6 ± 0.1

[a] Fractionation experiments were carried out treating 3 g of biomass (particle size < 2 mm) in 120 mL of an equivolumetric mixture of *n*-butanol and water, at 200 °C, under 30 bar of N_2 (introduced at ambient temperature), in the presence of $Na_2S_2O_4$ (16.7 % w/w), for a duration of 3 h. The reactions were carried out in duplicates.
[b] Expressed with respect to the weight of polysaccharide contained in the initial biomass.
[c] Expressed with respect to the weight of acid-insoluble lignin contained in the initial biomass.
[d] Expressed with respect to the amount of polysaccharide recovered in the pulp. The yields of saccharification of glucan and xylan for raw birch sawdust were 8% and 10%, respectively. For raw miscanthus they were 6% and 5%, respectively. For raw wheat straw they were 21% and 16%, respectively. For raw spruce sawdust they were 9% and 3%, respectively.
[e] The CI of raw birch sawdust was 49%. The CI of raw miscanthus was 64%. The CI of raw wheat straw was 63%. The CI of raw spruce sawdust was 62%.
[f] Non-condensed carbohydrate derivatives, expressed with respect to the total weight of polysaccharides contained in the initial biomass.

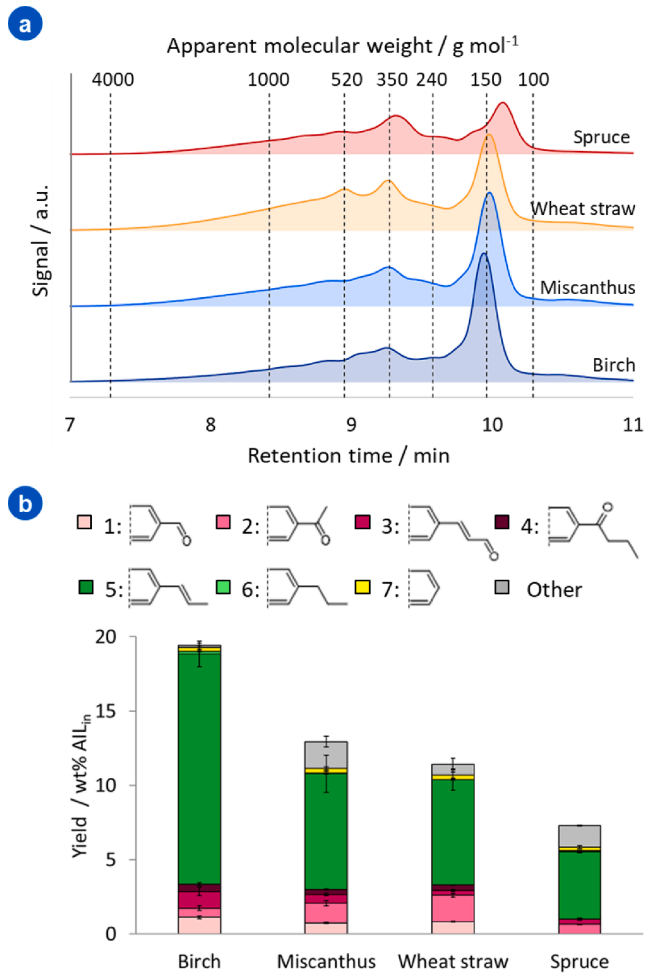


Fig. 7. Comparison of the GPC chromatograms (a), and of the yield of monophenolics as determined by GC (b) measured for the lignin oils isolated from the organic fractions obtained from the DAOF of different biomasses. Fractionation experiments were carried out treating 3 g of biomass in 120 mL of an equivolumetric mixture of *n*-butanol and water, at 200 °C, under 30 bar of N_2 (introduced at ambient temperature), in the presence of $Na_2S_2O_4$ (16.7 % w/$w_{biomass}$), for a duration of 3 h. The area underneath each chromatogram was normalized with respect to the yield of lignin oil obtained for the corresponding experiment. The monomer yield was calculated with respect to the acid insoluble lignin (AIL) content in the initial biomass.

4. Conclusions

In this contribution, a dithionite-assisted organosolv fractionation in *n*-butanol and water is discussed, for the one-pot production of cellulosic pulp and mono-/oligo-aromatics from lignocellulose. With the goal of highlighting potentially profitable process configurations, the effect of process conditions, including the operating temperature and pressure, the loading of dithionite, the solvent/biomass ratio, the reaction time, and the *n*-butanol/water ratio was investigated with respect to the properties of the isolated solid and liquid (organic and aqueous) fractions. Except for the exogenous N_2 pressure, all process variables were found to exert an influence on the yield and processability of the pulp, as well as on the yield of lignin oil and monophenolics. More specifically, the DAOF of birch wood performed at 200 °C for a duration of 3 to 6 h in a mixture of *n*-butanol and water resulted in the extensive removal of hemicellulose (up to ~ 90 wt%) and lignin (up to ~ 70 wt%) from the biomass, as well as in the near complete preservation of highly digestible cellulose. In parallel, a lignin oil was isolated from the organic fraction with remarkable yields (greater than84 wt% of acid insoluble lignin in the initial biomass), comprising phenolic monomers, dimers and oligomers. Importantly, the loading of dithionite was found to have a major impact on lignin depolymerization and on the yield of monophenolics, which reached a maximum of ~ 20 wt% of acid insoluble lignin (with a selectivity of 80 wt% for 4-propenyl-substituted monoaromatics), for a loading of 16.7 % w/$w_{biomass}$. On the other hand, the production of non-condensed carbohydrate derivatives in the aqueous fraction was found to be marginal for all the explored process configurations.

A techno-economic assessment of the DAOF highlighted that such technology may very well be economically viable, especially in wood-abundant regions. Apart for the cost of the raw biomass itself, the cost of sodium dithionite and *n*-butanol represent the largest contribution to operational costs. The economic potential of the DAOF was recognized to be strongly dependent on the market price of phenolic monomers and sensitivity analyses illustrated that a process configuration relying on a dithionite loading of 16.7 % w/$w_{biomass}$ and on the use of an equivolumetric mixture of *n*-butanol and water would be the most profitable.

Moreover, the treatment of lignocellulosic biomass from various sources revealed that the DAOF is a robust method, particularly suitable for processing hardwoods and herbaceous feedstocks, which resulted in high yields of digestible cellulosic pulp (with cellulose recoveries greater than 90 wt%) and depolymerized lignin oil (~90 wt% of acid insoluble lignin).

While alternative process configurations relying on less costly solvents (*e.g.* methanol, ethanol) and targeting the recovery and recycling of dithionite derivatives downstream should be envisaged, this study shows that the DAOF is a promising and relatively versatile method for integrating lignin valorization within biomass pretreatment, ultimately offering an innovative approach for the sustainable production of low-molecular weight aromatics from lignocellulose, in addition to a high-quality pulp.

Declaration of Competing Interest

The authors declare that they have no known competing financial interests or personal relationships that could have appeared to influence the work reported in this paper.

Data availability

Data will be made available on request.

Acknowledgements

This work was funded by an FSR grant (Fonds spéciaux de recherche) from UCLouvain and by the Innoviris research grant BRIDGE-RE4BRU. D. P. D. thanks the Francqui Foundation for his Francqui Research Professor Chair. K. V. A. acknowledges funding through FWO-SBO project BioWood and Catalisti-SBO project NIBCON. M. T. has received funding from the Research Foundation Flanders (FWO)-SBO BIOWOOD project. P.N. has received funding from the Energy Transition Fund ADV_BIO project, funded by the Belgian Federal Government's Department of Economy, General Direction of Energy. The MOCA platform of UCLouvain is acknowledged for its support with analytical techniques. M. Leclercq and T. Nicolay are acknowledged for their help with assembling the experimental setup and with the development of GC-MS/FID methods. E. Devos is acknowledged for performing ICP-AES analyses.

Appendix A. Supplementary data

Supplementary data to this article can be found online at https://doi.org/10.1016/j.cej.2022.138179.

References

[1] A.K. Chandel, V.K. Garlapati, A.K. Singh, F.A.F. Antunes, S.S. da Silva, Bioresour. Technol. 264 (2018) 370–381.
[2] M.V. Galkin, J.S.M. Samec, ChemSusChem 9 (2016) 1544–1558.
[3] J. Zakzeski, P.C.A. Bruijnincx, A.L. Jongerius, B.M. Weckhuysen, Chem. Rev. 110 (2010) 3552–3599.
[4] A.J. Ragauskas, G.T. Beckham, M.J. Biddy, R. Chandra, F. Chen, M.F. Davis, B. H. Davison, R.A. Dixon, P. Gilna, M. Keller, P. Langan, A.K. Naskar, J.N. Saddler, T. J. Tschaplinski, G.A. Tuskan, C.E. Wyman, Science 344 (2014) 1246843.
[5] A. Arevalo-Gallegos, Z. Ahmad, M. Asgher, R. Parra-Saldivar, H.M.N. Iqbal, Int. J. Biol. Macromol. 99 (2017) 308–318.
[6] M. Galbe, O. Wallberg, Biotechnol. Biofuels 12 (2019) 294.
[7] J. Baruah, B.K. Nath, R. Sharma, S. Kumar, R.C. Deka, D.C. Baruah, E. Kalita, Front. Energy Res. 6 (2018) 141.
[8] C. Ricardo Soccol, V. Faraco, S. Karp, L.P.S. Vandenberghe, V. Thomaz-Soccol, A. Woiciechowski, A. Pandey, *Biofuels*, Elsevier (2011) 101–122.
[9] S. Kang, J. Fu, G. Zhang, Renew. Sustain. Energy Rev. 94 (2018) 340–362.
[10] C. Xu, E. Paone, D. Rodríguez-Padrón, R. Luque, F. Mauriello, Chem. Soc. Rev. 49 (2020) 4273–4306.
[11] Y. Liao, S.-F. Koelewijn, G. Van den Bossche, J. Van Aelst, S. Van den Bosch, T. Renders, K. Navare, T. Nicolaï, K. Van Aelst, M. Maesen, H. Matsushima, J. M. Thevelein, K. Van Acker, B. Lagrain, D. Verboekend, B.F. Sels, Science 367 (2020) 1385–1390.
[12] W. Schutyser, S. Van den Bosch, J. Dijkmans, S. Turner, M. Meledina, G. Van Tendeloo, D.P. Debecker, B.F. Sels, ChemSusChem 8 (2015) 1805–1818.
[13] A. Deneyer, E. Peeters, T. Renders, S. Van den Bosch, N. Van Oeckel, T. Ennaert, T. Szarvas, T.I. Korányi, M. Dusselier, B.F. Sels, Nat. Energy 3 (2018) 969–977.
[14] R. Rinaldi, R. Jastrzebski, M.T. Clough, J. Ralph, M. Kennema, P.C.A. Bruijnincx, B. M. Weckhuysen, Angew. Chem. Int. Ed. 55 (2016) 8164–8215.
[15] W. Schutyser, T. Renders, S. Van den Bosch, S.-F. Koelewijn, G.T. Beckham, B. F. Sels, Chem. Soc. Rev. 47 (2018) 852–908.
[16] R.E. Key, J.J. Bozell, ACS Sustainable Chem. Eng. 4 (2016) 5123–5135.
[17] S. Van den Bosch, S.-F. Koelewijn, T. Renders, G. Van den Bossche, T. Vangeel, W. Schutyser, B.F. Sels, Top Curr Chem (Z) 376 (2018) 36.
[18] Z. Sun, B. Fridrich, A. de Santi, S. Elangovan, K. Barta, Chem. Rev. 118 (2018) 614–678.
[19] M. Wang, F. Wang, Adv. Mater. 31 (2019) 1901866.
[20] P. Azadi, O.R. Inderwildi, R. Farnood, D.A. King, Renew. Sustain. Energy Rev. 21 (2013) 506–523.
[21] X. Liu, F.P. Bouxin, J. Fan, V.L. Budarin, C. Hu, J.H. Clark, ChemSusChem 13 (2020) 4296–4317.
[22] M.M. Abu-Omar, K. Barta, G.T. Beckham, J.S. Luterbacher, J. Ralph, R. Rinaldi, Y. Román-Leshkov, J.S.M. Samec, B.F. Sels, F. Wang, Energy Environ. Sci. (2021) 262–292.
[23] Y.M. Questell-Santiago, M.V. Galkin, K. Barta, J.S. Luterbacher, Nat. Rev. Chem. 4 (2020) 311–330.
[24] X. Luo, Y. Li, N.K. Gupta, B. Sels, J. Ralph, L. Shuai, Angew. Chem. 132 (2020) 11800–11812.
[25] T. Renders, S. Van den Bosch, S.-F. Koelewijn, W. Schutyser, B.F. Sels, Energy Environ. Sci. 10 (2017) 1551–1557.
[26] T. Renders, G. Van den Bossche, T. Vangeel, K. Van Aelst, B. Sels, Curr. Opin. Biotechnol. 56 (2019) 193–201.
[27] E. Cooreman, T. Vangeel, K. Van Aelst, J. Van Aelst, J. Lauwaert, J.W. Thybaut, S. Van den Bosch, B.F. Sels, Ind. Eng. Chem. Res. 59 (2020) 17035–17045.
[28] S. Van den Bosch, T. Renders, S. Kennis, S.-F. Koelewijn, G. Van den Bossche, T. Vangeel, A. Deneyer, D. Depuydt, C.M. Courtin, J.M. Thevelein, W. Schutyser, B. F. Sels, Green Chem. 19 (2017) 3313–3326.
[29] G.E. Klinger, Y. Zhou, J.A. Foote, A.M. Wester, Y. Cui, M. Alherech, S.S. Stahl, J. E. Jackson, E.L. Hegg, ChemSusChem 13 (2020) 4394–4399.
[30] G.E. Klinger, Y. Zhou, P. Hao, J. Robbins, J.M. Aquilina, J.E. Jackson, E.L. Hegg, ChemSusChem 12 (2019) 4775–4779.
[31] Z. Fang, M.G. Flynn, J.E. Jackson, E.L. Hegg, Green Chem. 23 (2021) 412–421.
[32] F. Brienza, K. Van Aelst, K. Thielemans, B.F. Sels, D.P. Debecker, I. Cybulska, Green Chem. 23 (2021) 3268–3276.
[33] I. Cybulska, F. Brienza, D. P. Debecker, *Process for Producing Lignin Components from Lignocellulosic Biomass*, **2021**, WO2021058483.
[34] N.E. Thornburg, M.B. Pecha, D.G. Brandner, M.L. Reed, J.V. Vermaas, W. E. Michener, R. Katahira, T.B. Vinzant, T.D. Foust, B.S. Donohoe, Y. Román-Leshkov, P.N. Ciesielski, G.T. Beckham, ChemSusChem 13 (2020) 4495–4509.
[35] I. Cybulska, T. Chaturvedi, M. H. Thomsen, in *Biorefinery* (Eds.: J.-R. Bastidas-Oyanedel, J.E. Schmidt), Springer International Publishing, Cham, **2019**, pp. 153–165.
[36] Y. Kawamata, T. Yoshikawa, Y. Nakasaka, Y. Koyama, E. Fumoto, S. Sato, T. Tago, T. Masuda, J. Jpn. Pet. Inst. 62 (2019) 37–44.
[37] N. Paksung, Y. Matsumura, Ind. Eng. Chem. Res. 54 (2015) 7604–7613.
[38] Q. Jing, X. Lü, Chin. J. Chem. Eng. 15 (2007) 666–669.
[39] R.J.A. Gosselink, J.E.G. van Dam, F.H.A. Zomers, J. Wood Chem. Technol. 15 (1995) 1–25.
[40] W. Schutyser, S. Van den Bosch, T. Renders, T. De Boe, S.-F. Koelewijn, A. Dewaele, T. Ennaert, O. Verkinderen, B. Goderis, C.M. Courtin, B.F. Sels, Green Chem. 17 (2015) 5035–5045.
[41] L. Shuai, J. Luterbacher, ChemSusChem 9 (2016) 133–155.
[42] D.T. Balogh, A.A.S. Curvelo, R.A.M.C. De Groote, Holzforschung 46 (1992) 343–348.
[43] D. Crocker, D. Templeton, J. Sluiter, C. Scarlata, R. Ruiz, B. Hames, A. Sluiter, Determination of Structural Carbohydrates and Lignin in Biomass, National Renewable Energy Laboratory, Golden, CO, USA, 2012.
[44] L. Segal, J.J. Creely, A.E. Martin, C.M. Conrad, Text. Res. J. 29 (1959) 786–794.
[45] M. Selig, N. Weiss, Y. Ji, Enzymatic Saccharification of Lignocellulosic Biomass, National Renewable Energy Laboratory, Golden, CO, USA, 2008.
[46] K. Karimi, M.J. Taherzadeh, Bioresour. Technol. 200 (2016) 1008–1018.
[47] F. Hu, S. Jung, A. Ragauskas, Bioresour. Technol. 117 (2012) 7–12.
[48] Q. Schmetz, H. Teramura, K. Morita, T. Oshima, A. Richel, C. Ogino, A. Kondo, ACS Sustainable Chem. Eng. 7 (2019) 11069–11079.
[49] S.D. Shinde, X. Meng, R. Kumar, A.J. Ragauskas, Green Chem. 20 (2018) 2192–2205.
[50] N. Kobayashi, N. Okada, A. Hirakawa, T. Sato, J. Kobayashi, S. Hatano, Y. Itaya, S. Mori, Ind. Eng. Chem. Res. 48 (2009) 373–379.
[51] U. Agarwal, R. Atalla, in *Lignin and Lignans* (Eds.: C. Heitner, D. Dimmel, J. Schmidt), CRC Press, **2010**, pp. 103–136.
[52] C. Li, G. Cheng, V. Balan, M.S. Kent, M. Ong, S.P.S. Chundawat, L. daCosta Sousa, Y.B. Melnichenko, B.E. Dale, B.A. Simmons, S. Singh, Bioresour. Technol. 102 (2011) 6928–6936.
[53] F. Xu, J. Yu, T. Tesso, F. Dowell, D. Wang, Appl. Energy 104 (2013) 801–809.
[54] C. Fang, J.E. Schmidt, I. Cybulska, G.P. Brudecki, C.G. Frankær, M.H. Thomsen, Biomed Res. Int. 2015 (2015) 1–13.
[55] Q. Sun, M. Foston, X. Meng, D. Sawada, S.V. Pingali, H.M. O'Neill, H. Li, C. E. Wyman, P. Langan, A.J. Ragauskas, R. Kumar, Biotechnol. Biofuels 7 (2014) 150.
[56] W.-C. Tu, L. Weigand, M. Hummel, H. Sixta, A. Brandt-Talbot, J.P. Hallett, Cellulose 27 (2020) 4745–4761.
[57] Y. Liao, B.O. de Beeck, K. Thielemans, T. Ennaert, J. Snelders, M. Dusselier, C. M. Courtin, B.F. Sels, Molecular Catalysis 487 (2020), 110883.
[58] G. Garrote, H. Domínguez, J. C. Parajó, *Holz als Roh- und Werkstoff* **2001**, *59*, 53–59.
[59] S. Viamajala, B. S. Donohoe, S. R. Decker, T. B. Vinzant, M. J. Selig, M. E. Himmel, M. P. Tucker. In: O.V. Singh, S.P. Harvey (Eds.), *Sustainable Biotechnology*. Springer Netherlands, Dordrecht, **2010**, pp. 1–18.
[60] U.P. Agarwal, R.R. Reiner, S.A. Ralph, J. Agric. Food Chem. 61 (2013) 103–113.
[61] S. Van den Bosch, W. Schutyser, R. Vanholme, T. Driessen, S.-F. Koelewijn, T. Renders, B. De Meester, W.J.J. Huijgen, W. Dehaen, C.M. Courtin, B. Lagrain, W. Boerjan, B.F. Sels, Energy Environ. Sci. 8 (2015) 1748–1763.
[62] M.N. Borand, F. Karaosmanoğlu, J. Renew. Sustain. Energy 10 (2018), 033104.
[63] R. Rinaldi, R. Woodward, P. Ferrini, H. Rivera, J. Braz. Chem. Soc. (2018), https://doi.org/10.21577/0103-5053.20180231.
[64] I. van Zandvoort, Y. Wang, C.B. Rasrendra, E.R.H. van Eck, P.C.A. Bruijnincx, H. J. Heeres, B.M. Weckhuysen, ChemSusChem 6 (2013) 1745–1758.
[65] Z. Cheng, J.L. Everhart, G. Tsilomelekis, V. Nikolakis, B. Saha, D.G. Vlachos, Green Chem. 20 (2018) 997–1006.
[66] S.V. Makarov, Russ. Chem. Rev. 70 (2001) 885–895.
[67] S.V. Makarov, R. Silaghi-Dumitrescu, J. Sulfur Chem. 34 (2013) 444–449.
[68] P. Ferrini, R. Rinaldi, Angew. Chem. Int. Ed. 53 (2014) 8634–8639.
[69] K. Van Aelst, E. Van Sinay, T. Vangeel, E. Cooreman, G. Van den Bossche, T. Renders, J. Van Aelst, S. Van den Bosch, B.F. Sels, Chem. Sci. 11 (2020) 11498–11508.
[70] T. Renders, E. Cooreman, S. Van den Bosch, W. Schutyser, S.-F. Koelewijn, T. Vangeel, A. Deneyer, G. Van den Bossche, C.M. Courtin, B.F. Sels, Green Chem. 20 (2018) 4607–4619.
[71] P. Ferrini, C.A. Rezende, R. Rinaldi, ChemSusChem 9 (2016) 3171–3180.
[72] D.V. Evtuguin, in: N. Belgacem, A. Pizzi), John Wiley & Sons Inc, Hoboken, NJ, USA, 2016, pp. 225–244.
[73] H. Sixta (Ed.), in *Handbook of Pulp*, Wiley-VCH Verlag GmbH, Weinheim, Germany, 2006, pp. 366–509.
[74] H. Sixta, A. Potthast, A. W. Krotschek, in: H. Sixta Ed., *Handbook of Pulp*. Wiley-VCH Verlag GmbH, Weinheim, Germany, **2006**, pp. 109–229.
[75] M. Tschulkow, T. Compernolle, S. Van den Bosch, J. Van Aelst, I. Storms, M. Van Dael, G. Van den Bossche, B. Sels, S. Van Passel, J. Cleaner Prod. 266 (2020), 122022.
[76] A.W. Bartling, M.L. Stone, R.J. Hanes, A. Bhatt, Y. Zhang, M.J. Biddy, R. Davis, J. S. Kruger, N.E. Thornburg, J.S. Luterbacher, R. Rinaldi, J.S.M. Samec, B.F. Sels, Y. Román-Leshkov, G.T. Beckham, Energy Environ. Sci. 14 (2021) 4147–4168.
[77] D.M. Alonso, S.H. Hakim, S. Zhou, W. Won, O. Hosseinaei, J. Tao, V. Garcia-Negron, A.H. Motagamwala, M.A. Mellmer, K. Huang, C.J. Houtman, N. Labbé, D. P. Harper, C.T. Maravelias, T. Runge, J.A. Dumesic, Sci. Adv. 3 (2017) e1603301.
[78] S. Gillet, M. Aguedo, L. Petitjean, A.R.C. Morais, A.M. da Costa Lopes, R. M. Łukasik, P.T. Anastas, Green Chem. 19 (2017) 4200–4233.
[79] D. Wei Kit Chin, S. Lim, Y.L. Pang, M.K. Lam, Biofuels, Bioprod. Bioref. 14 (2020) 808–829.
[80] M. P. Ansell, in *Wood Composites*, Elsevier, **2015**, pp. 3–26.